Responses to the comments of Reviewer #2:

We would like to thank the anonymous referee for his/her comprehensive review and valuable suggestions. These suggestions help us to present our results more clearly. In response, we have made changes according to the referee's suggestions and replied to all comments point by point. All the page and line number for corrections are referred to the revised manuscript, while the page and line number from original reviews are kept intact.

1. Lines 33–35 and 548–550: Regarding the conclusion that this study's top-down emission inversion is lower compared to others, the authors mainly attribute this to the higher resolution used here, which captures finer emission details—a point supported by comparing results from the inner and outer nested domains. While this explanation is reasonable, it may not be entirely sufficient. Other factors like differences in methods, models, and observations—including how chemical processes, soil sinks, and boundary conditions are represented—could also contribute significantly. It would be good if the authors could briefly discuss these aspects in the Discussion.

Response: Thank you for this insightful comment. We agree that factors beyond spatial resolution, including representations of chemical processes, soil sinks, and boundary conditions, could influence top-down emission inversion results. First, regarding soil sinks, the flux of CH_4 uptake by soils in China is relatively small. According to the Global Methane Budget report, the latest bottom-up soil sink results for China in 2020 are 1.9-2.3 $Tg \cdot yr^{-1}$, while the top-down inversion results are 1.2-2.7 $Tg \cdot yr^{-1}$ (Saunois et al., 2025). Thus, uncertainties associated with soil sinks have a negligible influence on China's overall CH_4 emission estimates.

We also evaluated the impacts of other key factors on inversion results through sensitivity experiments (Figure R1). Using the default CAMS global concentration field (relative to adjusted fields) leads to a 7.5% increase in posterior emissions; adopting the CAMS-GLOB-ANT v6.2 inventory (instead of the base EDGAR inventory) as a

prior results in a 5.2% increase in posterior emissions; incorporating CH_4 chemical reactions (vs. omitting them) causes a 6.6% increase in posterior emissions; assimilating the TROPOMI/WFMD product (vs. TROPOMI/SRON) leads to a 4.4% increase in posterior emissions; and variations in assimilation system parameters (e.g., observation error, background error and local scale) have minimal impacts, limiting posterior emission changes to a range of -0.8% to 1.7%.

To further understand the extent to which different sensitivity factors affect our relatively low posterior emission results, we first compared the inversion results of the same experiment under the D02 domain coverage at different resolutions. Overall, we found that in the BASE experiment and all SENS experiments, emissions inverted at a 9 km resolution were typically 5.4–10.6% lower than those inverted at a 27 km resolution. This indicates that higher-resolution inversion consistently yields lower emission estimates. Second, we compared the emission differences between SENS experiments and the BASE experiment under the D02 domain coverage at the same 27 or 9 km resolution. It is important to note that only positive differences (i.e., SENS emissions > BASE emissions) can indicate that this factor, unaccounted for in the present study (i.e., the BASE scenario), may explain the low emission results observed in this study. For example, Figure R2 shows that, for grids within the D02 domain coverage, the emissions inverted in the SENS1 experiment increased by 5.1% and 4.3% compared with those in the BASE experiment at 27 km and 9 km resolutions, respectively. However, under the same D02 domain coverage (i.e., for the same set of grids), SENS1 showed that emissions inverted at 9 km resolution are 8.4% lower than those inverted at 27 km resolution. Overall, in every sensitivity experiment with a positive difference (SENS – BASE: 0.3–7.2%), the magnitude of this positive difference was smaller than the emission reduction caused by high-resolution inversion (9 km – 27 km: 5.4–10.6%) under the corresponding SENS experiment. This confirms that higher resolution remains the dominant driver of our lower inversion results relative to previous studies, while the aforementioned factors (chemical processes, boundary conditions, etc.) contribute secondary, manageable uncertainties. To address

this concern comprehensively, we have added the above discussion in the revised manuscript.

See Lines 676-713, Pages 31-34.

"To better evaluate the potential impact of prior uncertainties on posterior emission estimates, we conducted additional inversion experiments (SENS2) using the 2022 CAMS-GLOB-ANT v6.2 inventory as prior emissions. Nationwide, the posterior emissions in SENS2 increased by 5.2% compared with those in the BASE experiment. More importantly, the initial difference between the two prior inventories (6.0 Tg) converged to a much smaller difference of 2.3 Tg in the posterior results, indicating good robustness of the assimilation system at the national scale. However, in southern China (south of 30°N), due to limited observational constraints, the difference between the two prior inventories (5.8 Tg) only decreased to 4.8 Tg in the posterior results. In contrast, in observation-dense regions such as Shanxi Province, even though the difference in prior emissions was only 61.9 Gg, the difference in optimized posterior emissions further converged to 39.0 Gg.

Uncertainty in atmospheric transport models can contribute to model-data mismatch errors. Consistent with previous studies (Chen et al., 2022), this study initially omitted CH_4 chemical reactions to accelerate model integration and inversion efficiency. To quantify the impact of this simplification, we further conducted an additional inversion experiment (SENS3) where CH_4 chemical reactions were incorporated into the CMAQ model. Results showed that the inclusion of chemical reactions led to a 6.6% difference compared to the base experiment. Specifically, the difference was small in winter (only 1.7%), whereas in summer, the OH concentration in the lower troposphere was one order of magnitude higher than that in winter (Lelieveld et al., 2016). This stronger OH-driven CH_4 oxidation resulted in an increase of over 10% in posterior emissions. This indicates that accounting for CH_4 chemical reactions in summer is still necessary for accurate emission inversion. The impact of chemical reactions only increased emission estimates by 1.9% in Shanxi Province.

Different satellite products employ distinct inversion algorithms, which in turn determine the quality and quantity of the data. To assess how satellite product selection influences emission inversion, the TROPOMI/WFMD product was assimilated in SENS4. Compared with the operational TROPOMI product in BASE experiment, the TROPOMI/WFMD product provided a 59.3% increase in the number of observations, particularly notable in winter. In mainland China, posterior emissions derived from SENS4 increased by 4.4%, primarily driven by higher emission estimates in March and April. In Shanxi Province, posterior emissions showed a more modest increase of 2.2%.

Our results may also be subject to several uncertainties associated with the settings of assimilation system parameters. In particular, background and observation errors influence the weight assigned to prior emissions versus observations in determining posterior emissions, while the localization scale dictates the distance over which observational information affects the inversion results. To quantify these impacts, we conducted sensitivity tests by adjusting key parameters: observation errors were set to 0.5% and 0.9% (SENS5-6), background errors to 30% and 50% (SENS7-8), and localization scales to 250 km and 350 km (SENS9-10), respectively. However, our sensitivity analysis revealed that varying these parameters, whether increasing or decreasing their values, only led to differences of -0.7% to 1.7% in posterior emission estimates across mainland China. This indicates that the CH_4 emission estimates were not significantly affected by adjustments to the system parameters."

See Lines 739-752, Pages 34-35.

"Our inversion results are generally lower than previous emission estimates… …we found that emissions inverted at a 9 km resolution were typically 5.4-10.6% lower than those at a 27 km resolution. This indicates that higher-resolution inversion consistently yields lower emission estimates, a discrepancy likely driven by the fact that higher-resolution simulations excel at capturing localized emission hotspots that lead to elevated concentration values… ... To further understand the extent to which different sensitivity factors affect our relatively low posterior emission results, we compared the emission differences between SENS experiments and the BASE experiment under the

inner domain coverage at the same 27 or 9 km resolution (Figure R7). In every sensitivity experiment with a positive difference (SENS – BASE), the magnitude varies between 0.3-7.2%, which is always smaller than the emission reduction caused by high-resolution inversion under the corresponding SENS experiment. This confirms that higher resolution remains the dominant driver of our lower inversion results relative to previous studies, while the aforementioned factors contribute to secondary, manageable uncertainties… …"

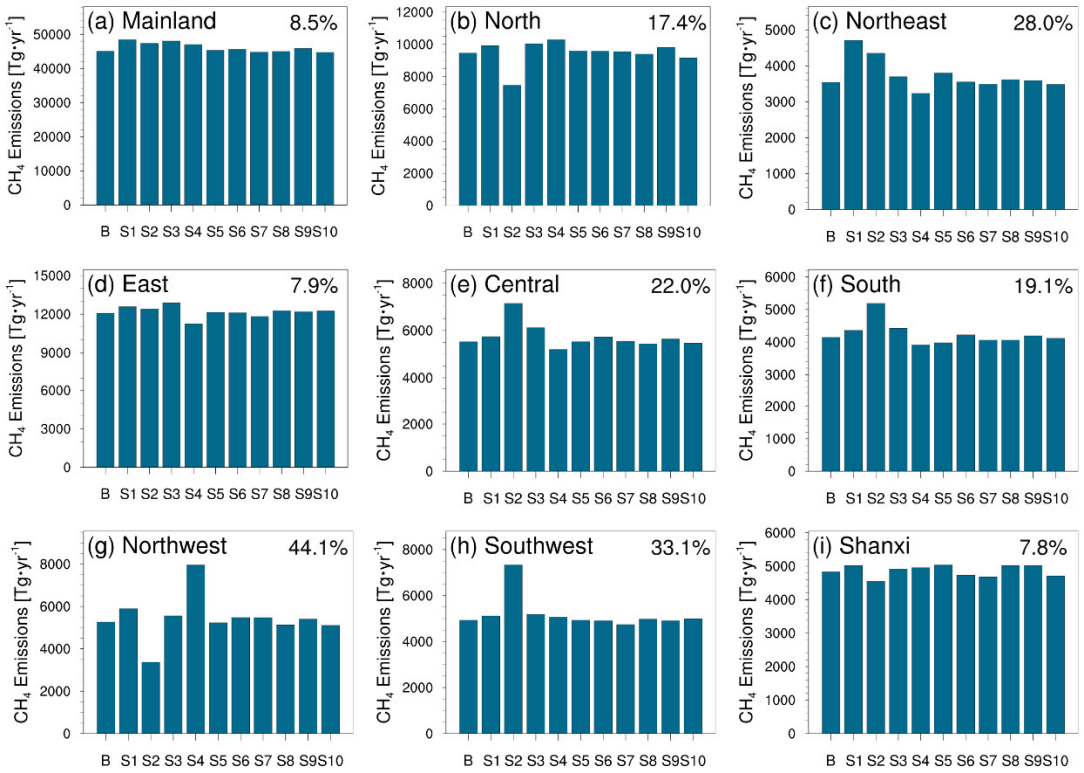

Figure R1 Posterior CH_4 emissions from the base and different sensitivity experiments (Table S6). B denotes the BASE experiment. S1 to S10 denote the SENS1 to SENS10 experiments, respectively. Posterior CH_4 emissions from the base and different sensitivity experiments. B denotes the BASE experiment. S1 to S10 denote the SENS1 to SENS10 experiments, respectively. S1 represents the experiment using the unadjusted CAMS global concentration field as the boundary; S2 denotes the experiment adopting CAMS-GLOB-ANT v6.2 inventory as the prior emission inventory; S3 denotes the inversion experiment accounting for CH_4 chemical reactions; S4 denotes the inversion experiment assimilating the TROPOMI/WFMD product; S5

and S6 denote the experiments with observation errors set to 0.5% and 0.9%, respectively; S7 and S8 denote the experiments with background errors set to 30% and 50%, respectively; S9 and S10 denote the experiments with the localization scale adjusted to 250 km and 350 km, respectively. The numbers on the figure represent the uncertainty values of different regions. The numbers on the figure represent the uncertainty values of different regions. (Figure 8 in the revised manuscript)

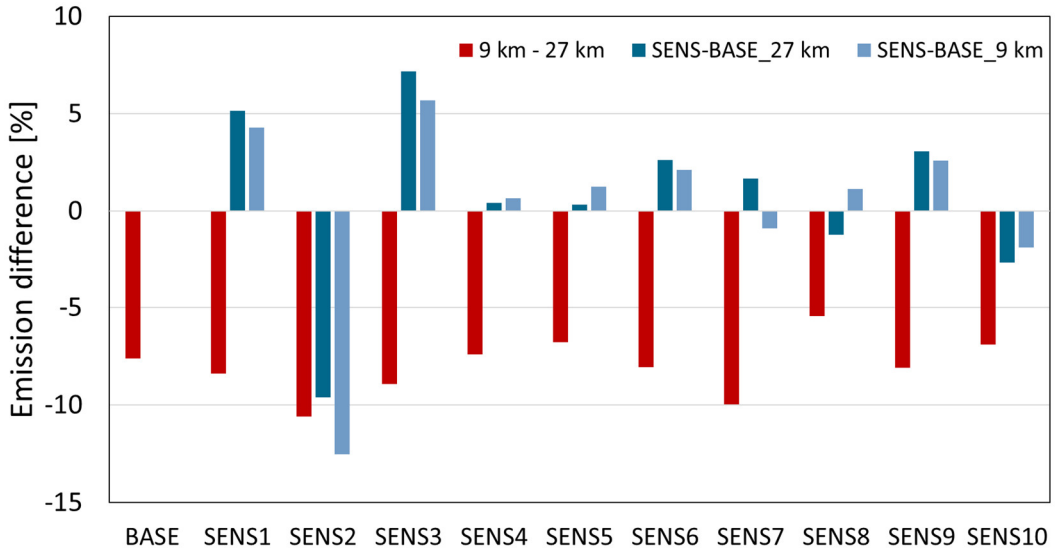

Figure R2 Comparison of emission differences under the D02 domain coverage: one between 9 km and 27 km resolutions within the same BASE or SENS experiment (red), and the other between corresponding SENS and BASE experiments at either 27 km (dark blue) or 9 km (light blue) resolution. Note that only positive differences (i.e., SENS > BASE emissions) can indicate unconsidered factors that might lead to the low emission results in our study. (Figure S7 in the Supplementary Information)

2. Figure 1b: It shows that TROPOMI data has a high missing rate across the country, especially in the south, with some areas having coverage for only 10% of the dates. For regions with long periods of no observation, how are the posterior emissions represented? Also, what is the impact of this representation on daily, monthly and yearly CH4 emission estimates? It would be helpful if the authors could discuss this as well.

Response: Thank you for this comment. First, regarding the representation of posterior emissions in observation-sparse regions, our assimilation system addresses data gaps

through two key mechanisms. On one hand, the system not only optimizes grids with direct observations but also uses the atmospheric transport model to capture the source-receptor relationship between emissions from surrounding grids and CH_4 concentrations at observation sites, thereby enabling the optimization of emissions in surrounding grids within a 300 km localization scale. On the other hand, we adopt an iterative approach where emissions optimized in the current assimilation window serve as prior emissions for the next window, facilitating rolling assimilation to sustain the influence of observational information over time.

Therefore, at the daily scale, grids without observational constraints directly adopt emissions from the previous window. This approach may slightly underestimate short-term emission fluctuations but maintains temporal continuity in emission trends. At the monthly scale, grids with no continuous observational constraints throughout the month directly use EDGAR data. Such grids account for 7.9% of all grids and contribute 0.3% to total posterior emissions. While this may lead to insufficient observational constraints on posterior emissions, particularly in southern regions during summer, it effectively avoids seasonal distortions in posterior estimates caused by variations in emissions. At the annual scale, 4.8% of grids remain unadjusted, and the unadjusted emissions in these grids are mainly distributed in uninhabited areas of Southwest China, resulting in a negligible overall impact (0.00037%) on annual CH_4 emission estimates.

To further verify the robustness of our emission optimization under limited observations, we conducted additional sensitivity experiments (e.g., SENS2, detailed in Response to Comment 1) where we compared the impact of different prior inventories on posterior emission estimates. We have added the following discussion in the revised manuscript. See Lines 305-319, Page 13.

"For regions with limited observation coverage (e.g., southern China), posterior emission estimates may rely heavily on prior information (see Discussion). On one hand, the system optimizes emissions in grids surrounding observations through the source-receptor relationship of atmospheric transport, allowing it to impose extensive constraints on emissions (Figure S4); on the other hand, it adopts an iterative approach

where emissions optimized in the current window serve as prior emissions for the next window, facilitating rolling assimilation and thereby sustaining the influence of observational information on emission estimates. However, intermittent observations may cause posterior emissions to underestimate short-term emission fluctuations. At the monthly scale, grids without continuous observational constraints throughout the month directly use EDGAR data. Such grids account for 7.9% of all grids and contribute 0.3% to total posterior emissions. Although this may lead to insufficient observational constraints on posterior emissions, particularly in southern regions during summer, it effectively avoids seasonal distortions in posterior estimates caused by variations in emissions. At the annual scale, 4.8% of grids remain unadjusted. These unadjusted emissions are mainly distributed in uninhabited areas of Southwest China, resulting in a negligible overall impact on annual CH_4 emission estimates."

3. Figure 3 on page 20 shows the differences in prior and posterior emissions for different sectors. How are the sectors distinguished in the posterior emissions? It is indeed challenging to differentiate sectoral emissions in top-down emission inversion. Typically, sectoral emissions in the posterior are calculated based on the proportional grid emissions from the prior inventory. Does this study use the same method?

Response: Thank you for this comment. Yes, that's correct. Following Kou et al. (2025), Zhang et al. (2022), and Miller et al. (2019), we partitioned the optimized total emissions based on the prior proportional information of different sectors within the same model grid. This method is adopted because the observed total atmospheric CH_4 concentration integrates emission signals from all sectors, making it difficult to distinguish emission information from different source sectors overlapping in a pixel grid (Saunois et al., 2025). As a result, the emissions derived directly from our inversion represent the total CH_4 flux at the pixel scale. We acknowledge that uncertainties may be introduced into posterior sectoral statistics by potential errors in the sectoral proportionality of the prior inventory, and this limitation is noted in the revised manuscript.

See Lines 377-381, Pages 16-17.

"Assimilating total CH_4 observations alone cannot disentangle emissions from different source sectors overlapping in individual grid cells (Saunois et al., 2025). Consequently, we partitioned the inversion results into respective emission sectors based on the monthly prior proportions at the model grid points (Kou et al., 2025; Zhang et al., 2022), though this approach does introduce a certain degree of uncertainty in sectoral attribution. The sectoral patterns offer insights into the underlying factors influencing China's emission changes. We concentrated on interpreting the emissions from the coal, gas, rice cultivation… …"

4. The title of Figure 4 needs to specify the time period covered by the data. Is it the average for the entire year of 2022?

Response: Yes. Figure 4 presents the evaluation of XCH_4 averaged over the entire year of 2022. We have supplemented the time information in the figure caption to clarify this detail.

See Line 560, Page 24.

"**Figure 4** Comparison of simulated XCH_4 (ppb) from prior and posterior emissions with TROPOMI observations over (a-c) China and (d-f) Shanxi Province for the 2022 annual average."

5. On line 509, P24, 'Except for LF site...', this description is incorrect. Not only is the LF site underestimated, but the TY site is also significantly underestimated, as well as the JC site. It is recommended to correct the description."

Response: Thank you for pointing out this ambiguity in our description. The original intent was to highlight that the LF site showed a worsened bias, shifting to a severe negative bias and larger RMSE in VEP experiment (posterior simulations). Although the TY and JC sites still showed an underestimation in the VEP experiment, their overall

performance has improved in VEP experiment.

We have revised the sentence. See Lines 588-589, Page 26.

"Except for the LF site, which shifted to a severe negative bias and exhibited a larger RMSE, the VEP experiment demonstrated varying degrees of improvement at the other five sites."

References

Chen, Z., Jacob, D. J., Nesser, H., Sulprizio, M. P., Lorente, A., Varon, D. J., Lu, X., Shen, L., Qu, Z., Penn, E., and Yu, X.: Methane emissions from China: a high-resolution inversion of TROPOMI satellite observations, Atmos. Chem. Phys., 22, 10809-10826, 10.5194/acp-22-10809-2022, 2022.

Jiang, F., Wang, H., Chen, J. M., Ju, W., Tian, X., Feng, S., Li, G., Chen, Z., Zhang, S., Lu, X., Liu, J., Wang, H., Wang, J., He, W., and Wu, M.: Regional CO2 fluxes from 2010 to 2015 inferred from GOSAT XCO2 retrievals using a new version of the Global Carbon Assimilation System, Atmos. Chem. Phys., 21, 1963-1985, 10.5194/acp-21-1963-2021, 2021.

Kou, X., Peng, Z., Han, X., Li, J., Qin, L., Zhang, M., Parker, R. J., and Boesch, H.: China's methane emissions derived from the inversion of GOSAT observations with a CMAQ and EnKS-based regional data assimilation system, Atmospheric Pollution Research, 16, 102333, 10.1016/j.apr.2024.102333, 2025.

Miller, S. M., Michalak, A. M., Detmers, R. G., Hasekamp, O. P., Bruhwiler, L. M. P., and Schwietzke, S.: China's coal mine methane regulations have not curbed growing emissions, Nature Communications, 10, 303, 10.1038/s41467-018-07891-7, 2019.

Murguia-Flores, F., Arndt, S., Ganesan, A. L., Murray-Tortarolo, G., and Hornibrook, E. R. C.: Soil Methanotrophy Model (MeMo v1.0): a process-based model to quantify global uptake of atmospheric methane by soil, Geosci. Model Dev., 11, 2009-2032, 10.5194/gmd-11-2009-2018, 2018.

Nassar, R., Hill, T. G., McLinden, C. A., Wunch, D., Jones, D. B. A., and Crisp, D.: Quantifying CO2 Emissions From Individual Power Plants From Space, Geophysical Research Letters, 44, 10,045-010,053, 10.1002/2017GL074702, 2017.

Saunois, M., Martinez, A., Poulter, B., Zhang, Z., Raymond, P. A., Regnier, P., Canadell, J. G., Jackson, R. B., Patra, P. K., Bousquet, P., Ciais, P., Dlugokencky, E. J., Lan, X., Allen, G. H., Bastviken, D., Beerling, D. J., Belikov, D. A., Blake, D. R., Castaldi, S., Crippa, M., Deemer, B. R., Dennison, F., Etiope, G., Gedney, N., Höglund-Isaksson, L., Holgerson, M. A., Hopcroft, P. O., Hugelius, G., Ito, A., Jain, A. K., Janardanan, R., Johnson, M. S., Kleinen, T., Krummel,

P. B., Lauerwald, R., Li, T., Liu, X., McDonald, K. C., Melton, J. R., Mühle, J., Müller, J., Murguia-Flores, F., Niwa, Y., Noce, S., Pan, S., Parker, R. J., Peng, C., Ramonet, M., Riley, W. J., Rocher-Ros, G., Rosentreter, J. A., Sasakawa, M., Segers, A., Smith, S. J., Stanley, E. H., Thanwerdas, J., Tian, H., Tsuruta, A., Tubiello, F. N., Weber, T. S., van der Werf, G. R., Worthy, D. E. J., Xi, Y., Yoshida, Y., Zhang, W., Zheng, B., Zhu, Q., Zhu, Q., and Zhuang, Q.: Global Methane Budget 2000–2020, Earth Syst. Sci. Data, 17, 1873-1958, 10.5194/essd-17-1873-2025, 2025.

Zhang, Y., Fang, S., Chen, J., Lin, Y., Chen, Y., Liang, R., Jiang, K., Parker, R. J., Boesch, H., Steinbacher, M., Sheng, J.-X., Lu, X., Song, S., and Peng, S.: Observed changes in China's methane emissions linked to policy drivers, Proceedings of the National Academy of Sciences, 119, e2202742119, doi:10.1073/pnas.2202742119, 2022.